

New *Initial* Position Detection Technique for Three-Phase Brushless DC Motor *Without* Position and Current Sensors

Yen-Shin Lai, *Senior Member, IEEE*, Fu-San Shyu, and Shian Shau Tseng

Abstract—This paper presents a new detection technique of initial position for a three-phase brushless dc motor which does not require any current and position sensors, and thereby significantly reduces the cost. The fundamental principle of the technique is to determine the initial position of the permanent magnet by the time periods of discharge of stator windings, which are excited before discharge. As compared to previous approaches, the presented technique does not cause any rotation during detection, and it is therefore very promising for particular kinds of applications, which do not allow the motor to rotate potentially in the wrong direction during initial position detection, e.g., electrical vehicles. As compared to earlier techniques, the presented technique dramatically simplifies the detection procedures and cost. Experimental results derived from a field-programmable gate-array-based control system will be presented to demonstrate the feasibility of the presented technique.

Index Terms—Brushless dc motor (BLDCM).

I. INTRODUCTION

IN GENERAL, a three-phase brushless dc motor (BLDCM) consists of permanent magnet and excitation windings. The initial position of the permanent magnet and excitation decide the rotation direction at the moment of startup. Fig. 1 shows the structure of a particular kind of BLDCM. As shown in Fig. 1, the rotor of motor has 12 poles and the stator has nine slots, and the voltage is fed to the stator via a three-phase inverter as shown in Fig. 2. The dc-link voltage is connected to the stator windings to create a field, which is perpendicular to the rotor field produced by the permanent magnet, in order to derive maximum torque and the specified rotational direction. This feature is achieved by proper commutations of inverter, which acts as a commutator and brush of conventional dc motors, once the position of the permanent magnet is known.

Therefore, the initial position of permanent magnet should be clearly identified for proper commutation control to avoid potentially wrong direction of rotation at the moment of startup.

Paper IPCSD 02–083, presented at the 2002 Industry Applications Society Annual Meeting, Pittsburgh, PA, October 13–18, and approved for publication in the IEEE TRANSACTIONS ON INDUSTRY APPLICATIONS by the Industrial Drives Committee of the IEEE Industry Applications Society. Manuscript submitted for review June 1, 2002 and released for publication January 4, 2003. This work was supported by Hitachi Micro System Asia (HMSA) Pte. Ltd.

Y.-S. Lai and F.-S. Shyu are with the Department of Electrical Engineering, National Taipei University of Technology, Taipei 106, Taiwan, R.O.C. (e-mail: yslai@ntut.edu.tw).

S. H. Tseng was with the Department of Electrical Engineering, National Taipei University of Technology, Taipei 106, Taiwan, R.O.C. He is now with Machvision, Inc., Hsin Chu, Taiwan, R.O.C.

Digital Object Identifier 10.1109/TIA.2003.809450

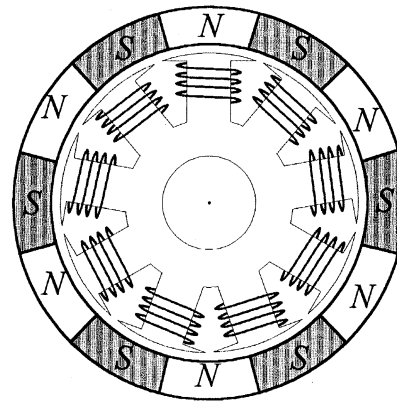


Fig. 1. Illustration of a BLDCM.

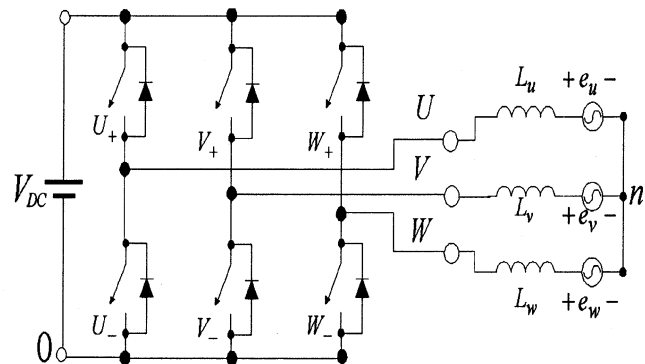


Fig. 2. Block diagram for a three-phase BLDCM drive.

Since the initial position detection of the BLDCM is essential for particular kinds of applications, such as an electrical scooter, several techniques [1]–[6] have been presented to detect the initial position of the BLDCM. Some of these techniques either require position sensors (Hall sensors) or current sensors, or may cause backward rotation.

To cope with the above-mentioned issues, this paper presents a novel initial position detection technique for BLDCM drives, which *does not* require any *current* and *position* sensors, and thereby significantly reduces the cost. Moreover, the presented technique *does not* cause any rotation during detection, and it is therefore very promising for particular kinds of applications, which do not allow the motor to rotate potentially in the *wrong* direction during initial position detection, e.g., electrical vehicles. As compared to the techniques shown in [4]–[6], the presented technique dramatically simplifies the

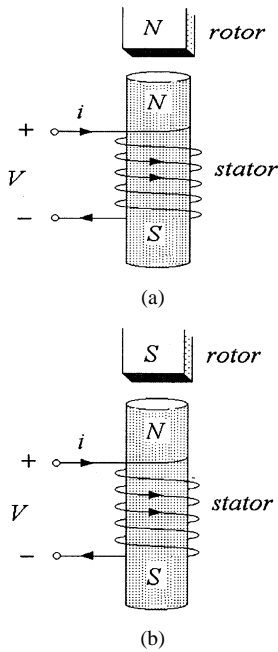


Fig. 3. Saturated and nonsaturated magnetic fields. (a) Linear (nonsaturated) magnetic field. (b) Saturated magnetic field.

detection procedures. Experimental results derived from an field-programmable-gate-array (FPGA)-based control system will be presented to demonstrate the feasibility of the presented technique.

The paper is organized as follows. First, the previous techniques for initial position detection of a three-phase BLDCM are introduced, and then the features of the presented technique are fully explored. Finally, experimental results are presented to confirm theoretical analysis and support our claims.

II. PREVIOUS INITIAL POSITION DETECTION TECHNIQUES OF BLDCM

The principle for initial position detection techniques shown in [4]–[6] will be explained by the relationship between the magnitude of inductance and resultant magnetic field. As shown in Fig. 3(a), the fields of stator and rotor are with 180° phase shift, and thereby result in *linear (nonsaturated)* magnetic field. In contrast, as shown in Fig. 3(b), the stator field and rotor field are *in phase*. Therefore, the magnetic field is enhanced and becomes *saturated* when a proper excitation signal is fed into the stator.

It is well known that the associated inductance of stator windings for the *linear (nonsaturated)* case shown in Fig. 3(a) is *greater* than that for the *saturated* case shown in Fig. 3(b). Fig. 4 clearly identifies the inductance for these two cases. As we know that the stator is at standstill during the process of initial position identification, *the inductance value is therefore decided by the position of rotor (field)*. This fact is then used for the detection of the initial position of the permanent magnet.

Applying a step voltage to the stator windings, the rising time of the current reflects the time constant of the stator windings, which is *smaller* for the saturated case as compared to that for the linear case. Fig. 5 shows the experimental results of stator

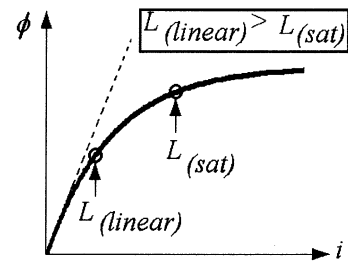


Fig. 4. Inductance of stator windings, depending upon the position of rotor

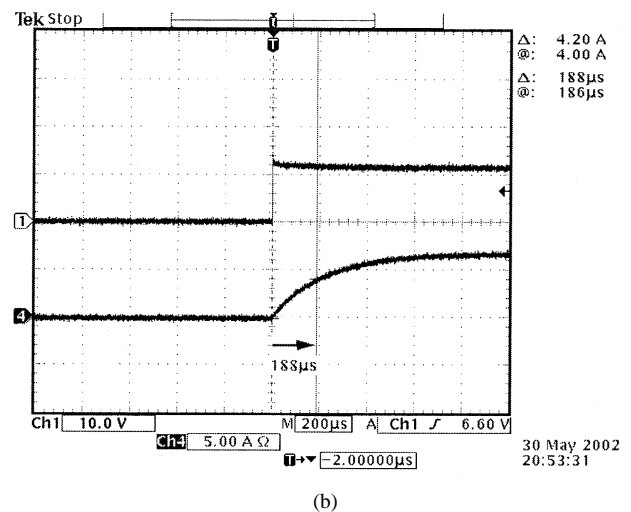
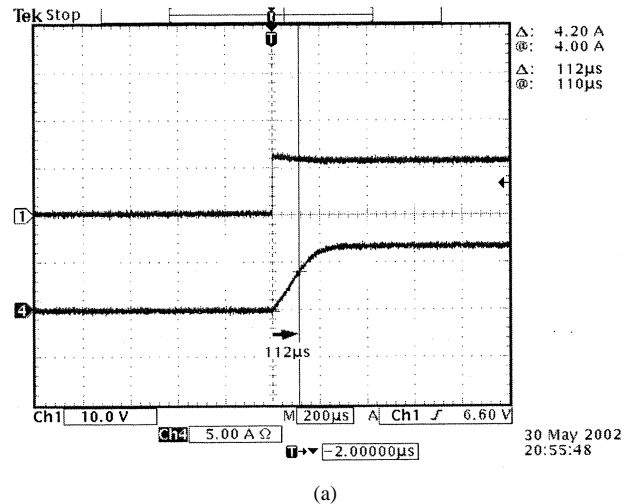


Fig. 5. Current response stator windings for linear and saturated cases. (a) Saturated case. (b) Nonsaturated case.

currents (lower trace) for a given applied voltage (upper trace). As shown in Fig. 5(a) for the case of *smaller* time constant, the current response is *faster* than that for Fig. 5(b) with *greater* time constant. Since the *rotor position* causes the difference of time constant, the response speed of stator current associated with the applied stator voltage pulse is, therefore, used to identify the initial position of rotor permanent magnet.

As shown in Fig. 6(a), excitation signals are applied to the stator windings for a short period, indicated by " t_p ," which is less than the time constant of the stator circuit. The *peak* values of the associated stator currents for different *excitation configurations* of stator windings are measured as shown in

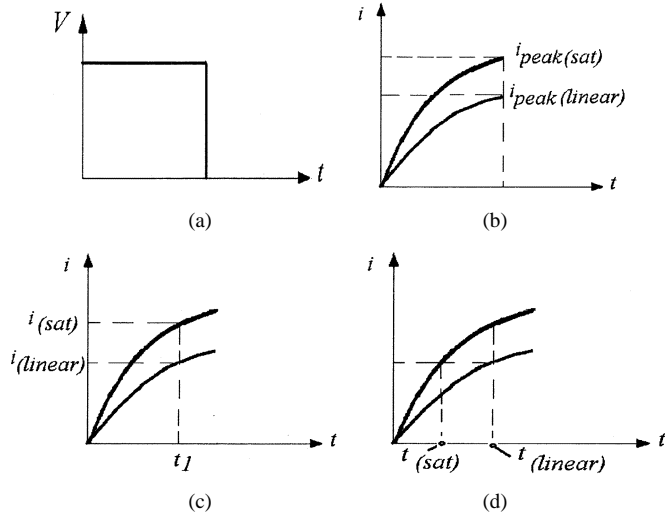


Fig. 6. Excitation voltage and the measured current for previous techniques [4]–[6]. (a) Excitation signal. (b) Current sensing for initial position detection [4]. (c) Current sensing for initial position detection [5]. (d) Current sensing for initial position detection [6].

Fig. 6(b). The position of the rotor permanent magnet is then determined by the comparison results, as shown in [4]. As shown in Fig. 6(b), the peak value for the saturated case is greater than that of the linear case.

Alternatively, for a given time, called “ t_1 ,” the *magnitudes* of stator currents shown in Fig. 6(c) for different excitation configurations are sensed to determine the position of the rotor permanent magnet [5]. As shown in Fig. 6(c), the current for the saturated case is greater than that for the linear case, as $t = t_1$.

The *response speed* of stator currents shown in Fig. 6(d) for different *excitation configurations* of stator windings can also be used to determine the position of the rotor permanent magnet [6]. As shown in Fig. 6(d), the response speed for the linear case is slower than that for the saturated case.

The excitation configurations of stator windings are changed by the excitation signals. Fig. 7 shows the excitation configurations for the initial position detection of the BLDCM [4]–[6]. As shown in Fig. 7, six procedures are required for the identification of the initial position of the permanent magnet.

Based upon this principle, several initial position detection techniques [4]–[6] for the BLDCM have been proposed. The initial position is identified within 180° by comparing the *peak*, *magnitude*, or *response speed*, of currents associated with the excitation signals shown in Fig. 7(a) and (b). Secondly, the range of initial position is determined within 120° by similar comparison results associated with the excitation signals shown in Fig. 7(c) and (d). Finally, the comparison results of the excitation signals shown in Fig. 7(e) and (f) are used to give the range of initial position within 60° .

III. PROPOSED INITIAL POSITION DETECTION TECHNIQUE FOR BLDCM [7]

A. Basic Principle

The principle for the presented initial position detection technique is also based upon the relationship between magnitude

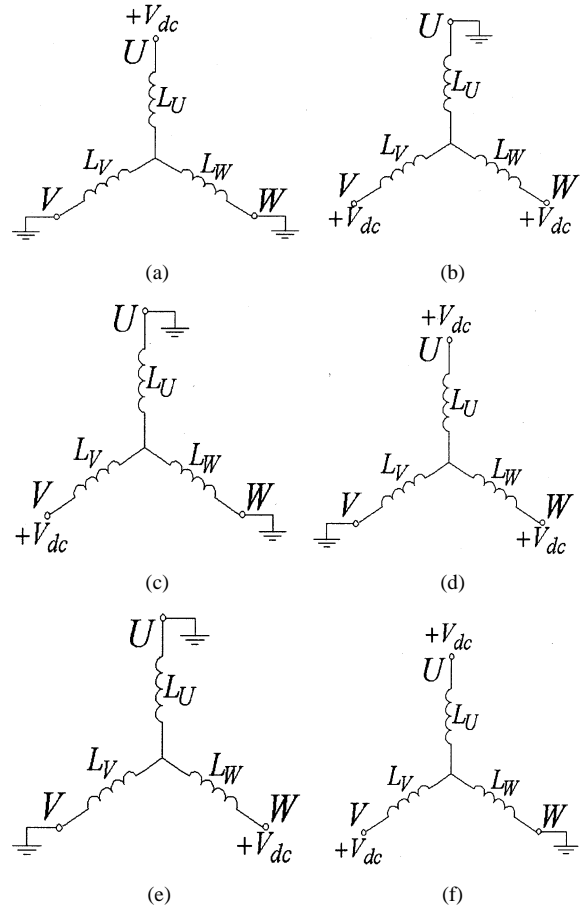


Fig. 7. Excitation configurations of conventional techniques [4]–[6].

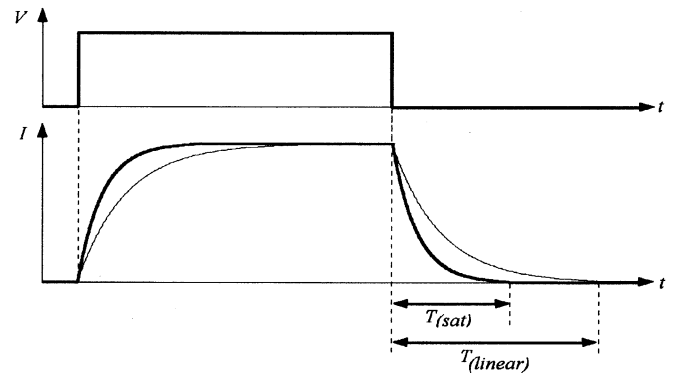


Fig. 8. Falling time of stator winding excited by a rectangular signal

of inductance and the resultant magnetic field. As shown in Fig. 3, the inductance magnitude shown in Fig. 3(a) for the saturation case is smaller than that of Fig. 3(b) for the nonsaturation one. Moreover, once the stator current reaches steady state after excitation, greater inductance stores more electric energy and thereby increases the falling time of *discharge* after the excitation signal is removed. Therefore, the falling period of the discharge process is used to identify the initial position of the rotor permanent magnet.

Fig. 8 shows the period of falling time of a stator winding excited by a rectangular signal. The resultant magnetic field of stator and rotor differs as rotor position changes, and thereby results in different inductance values and falling times. As shown

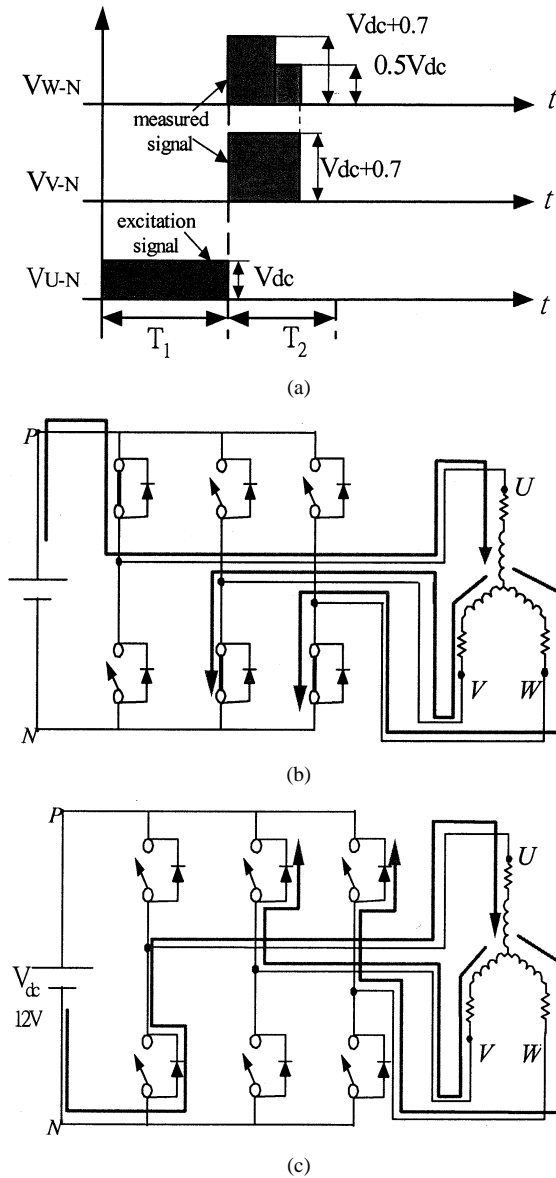


Fig. 9. Excitation configuration and the associated current path. (a) Illustration of excitation configuration. (b) Current path for t in " T_1 " period. (c) Current path for freewheeling period, t in " T_2 " period.

in Fig. 8, the period of falling time for the linear case is greater than that of the saturation case, $T_{\text{sat}} < T_{\text{linear}}$. The initial position is, therefore, identified according to the period of falling time of the stator windings.

B. Why Current Sensors Are Not Required

Fig. 9(a) illustrates one of the three configurations for excitation of the presented technique. For the excitation configuration as illustrated in Fig. 9(a), Fig. 9(b) shows the associated current path. As shown in Fig. 9(b), the current flows through the winding of phase " U ," and goes into the center-tap point of the stator windings. After that, the current passes through the stator windings of phase " V " and phase " W ," which are in parallel connection for this excitation configuration.

For t in the " T_2 " period, the main power devices are all turned off, and the current flows through the associated freewheeling diodes as shown in Fig. 9(c), without causing interruption of cur-

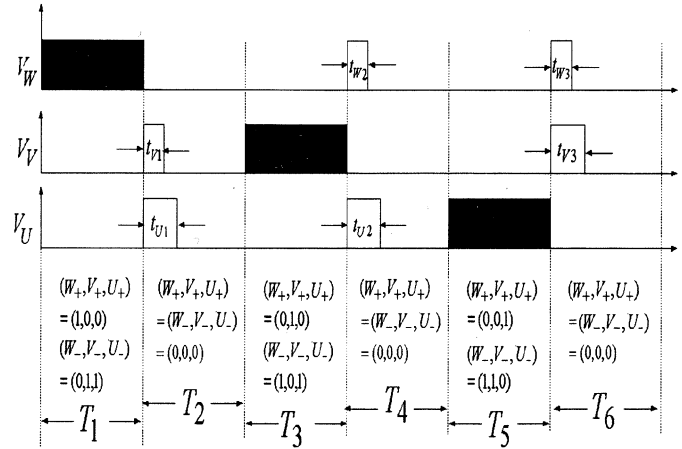


Fig. 10. Excitation signals and procedure for the presented technique.

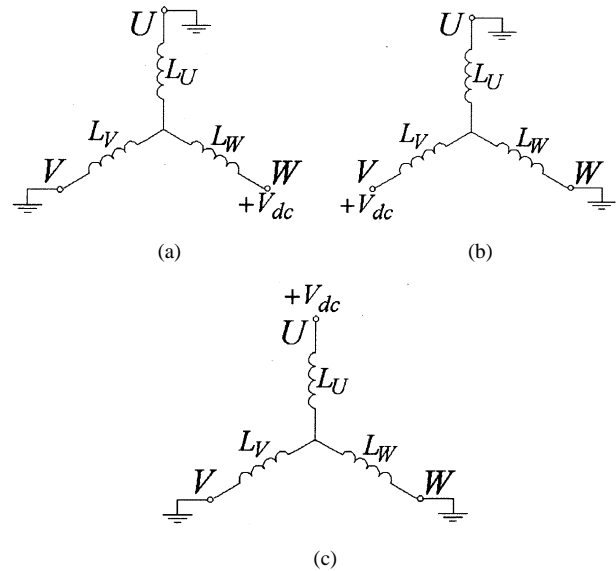


Fig. 11. Excitation of presented technique.

rent. The terminal voltage across the phase in the freewheeling state is equal to the $(V_{dc} + 0.7)$ V, as indicated in Fig. 9(c). Once the freewheeling period is over, this terminal voltage goes down and is approximately equal to $0.5V_{dc}$ V.

As discussed in the previous section, for the phase with *greater* inductance, it has a *longer* freewheeling period. Therefore, instead of detecting the peak, magnitude, or response time of *current*, only the *terminal voltage level* is used for the detection of the initial position of the permanent magnet. Therefore, *neither* current sensor *nor* position sensor is required for the presented technique.

Moreover, the terminal voltage is approximately equal to $(V_{dc} + 0.7)$ V, *despite* the magnitude of current during the identification process, and thereby simplifies the implementation. It will be shown later in this paper that no accurate A/D converter is required, and thereby a low-cost approach is provided.

C. New Technique for Initial Position Detection

Fig. 10 shows the excitation signals and procedure for the presented initial position detection technique. The associated

TABLE I
RELATIONSHIP BETWEEN INITIAL POSITION OF PERMANENT MAGNET AND THE IDENTIFICATION RESULTS

Identification Equations ("1" = Truth, "0" = False)				Initial Position
$t_{V3} - t_{W3} > 0$	$t_{W2} - t_{U2} > 0$	$t_{U1} - t_{V1} > 0$	$A = 2^2 X + 2^1 Y + 2^0 Z$	
$X=1$	$Y=0$	$Z=1$	$A=5$	$270^\circ\text{--}330^\circ$
$X=1$	$Y=0$	$Z=0$	$A=4$	$330^\circ\text{--}30^\circ$
$X=1$	$Y=1$	$Z=0$	$A=6$	$30^\circ\text{--}90^\circ$
$X=0$	$Y=1$	$Z=0$	$A=2$	$90^\circ\text{--}150^\circ$
$X=0$	$Y=1$	$Z=1$	$A=3$	$150^\circ\text{--}210^\circ$
$X=0$	$Y=0$	$Z=1$	$A=1$	$210^\circ\text{--}270^\circ$

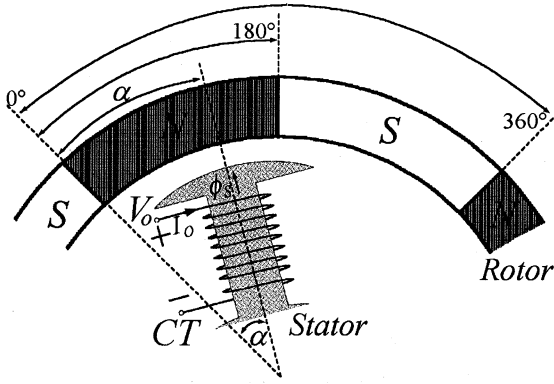


Fig. 12. Definition of initial position, "α" degrees; referring to "stator winding of phase U."

definition of main devices of the inverter is shown in Fig. 2. To highlight the simplification of the presented technique, Fig. 11 shows the excitation configurations of the motor in " T_1 ," " T_3 ," and " T_5 " time intervals as shown in Fig. 10. As shown in Figs. 10 and 11, the winding of the "W" phase is connected to the positive dc-link rail, and the windings of the "U" and "V" phases are connected to the negative one, during " T_1 " time interval. Then, the terminals voltage for the "V" and "U" phases are used for the detection of the initial position of the rotor permanent magnet.

The phase with *greater* resultant magnetic field has more stored energy, thereby resulting in a *longer freewheeling period* for the associated winding during the discharge process. Therefore, terminal voltages across the windings are measured instead of the current, for the identification of initial position. Of course, *neither* current sensor *nor* position sensor is required for the realization of the presented technique.

A similar process and remarks can also be derived for the other cases shown in Figs. 10 and 11. The relationship between the initial position of the permanent magnet and the identification results can be derived as shown in Table I; the definition associated with the position of the rotor permanent magnet is shown in Fig. 12.

As compared to previous techniques, the presented technique requires only three steps for excitation and significantly reduces the complexity of the identification process.

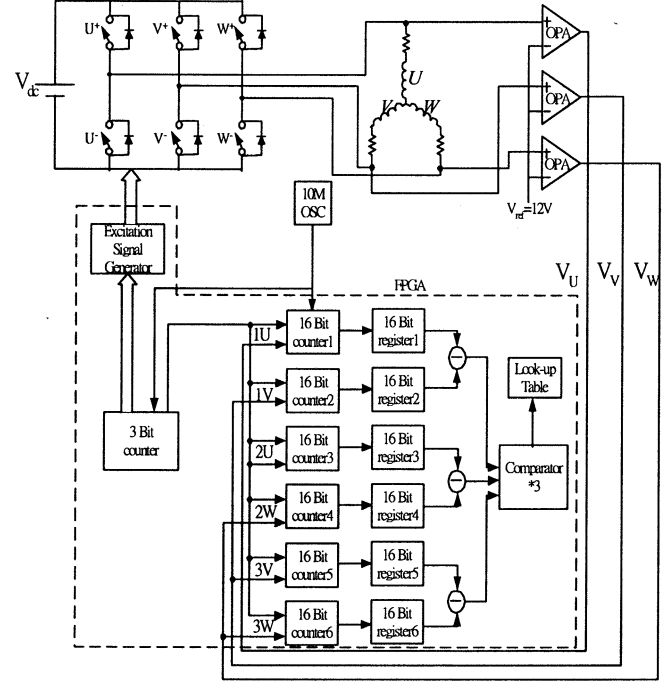


Fig. 13. Block diagram of experimental system.

TABLE II
FEATURES OF FPGA FOR IMPLEMENTATION

Feature	EPF6024
Typical gates	24,000
Logic elements (Les)	1,960
Maximum I/O pins	218
Supply voltage (V_{CCINT})	3.3V

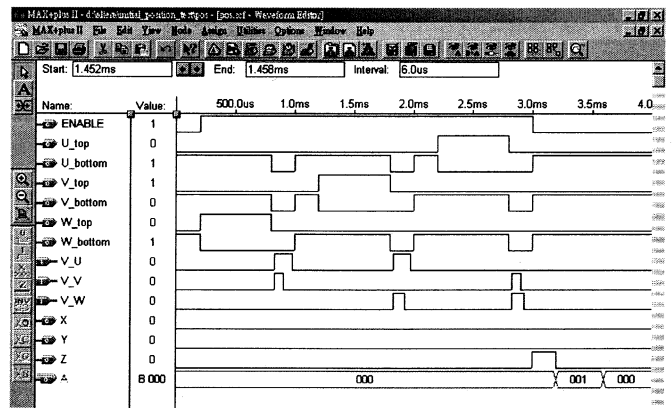


Fig. 14. Simulation results, "A" = 1.

IV. EXPERIMENTAL RESULTS

A. FPGA-Based Experimental System

Fig. 13 shows the experimental system, which consists of FPGA, a BLDCM, and the associated external circuits. Only terminal voltages of three phases are sampled and fed into the FPGA to identify the initial position of the permanent magnet.

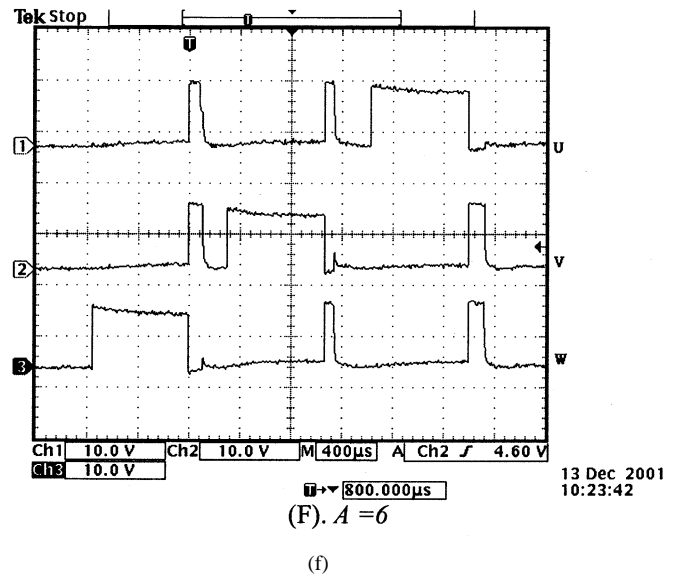
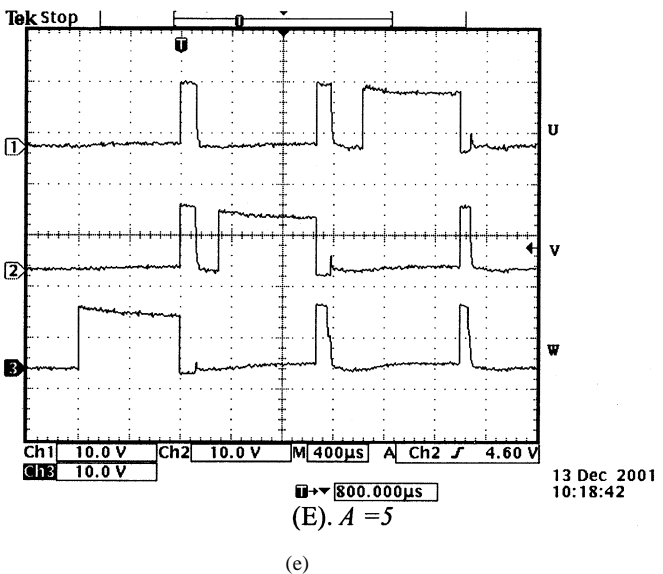
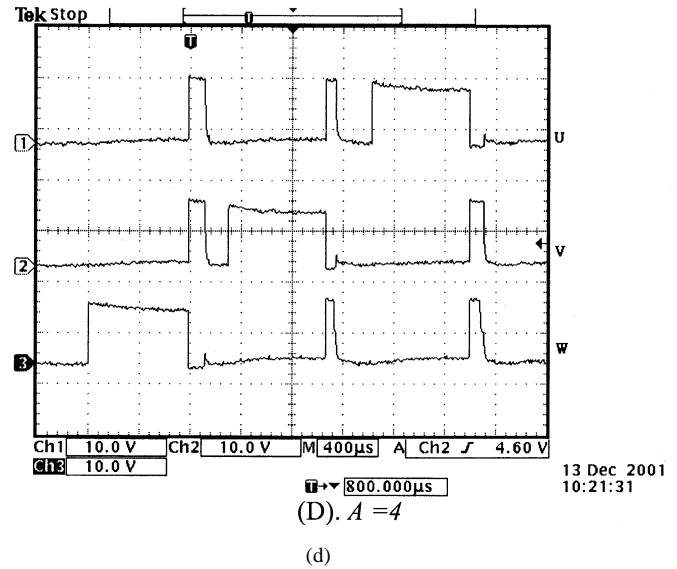
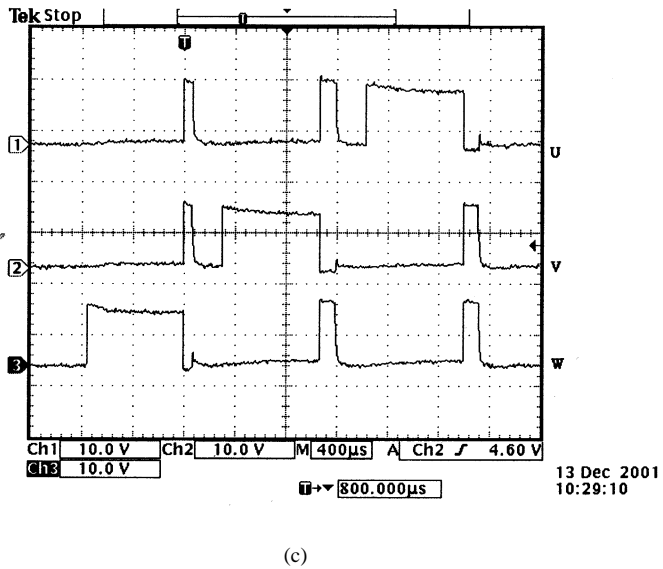
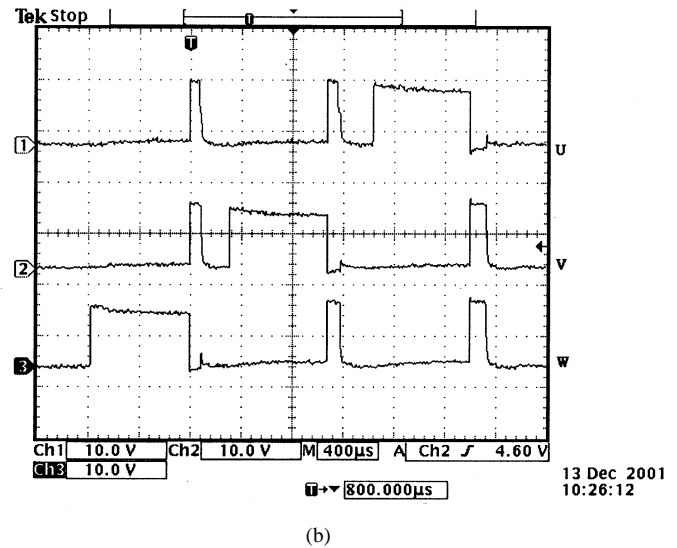
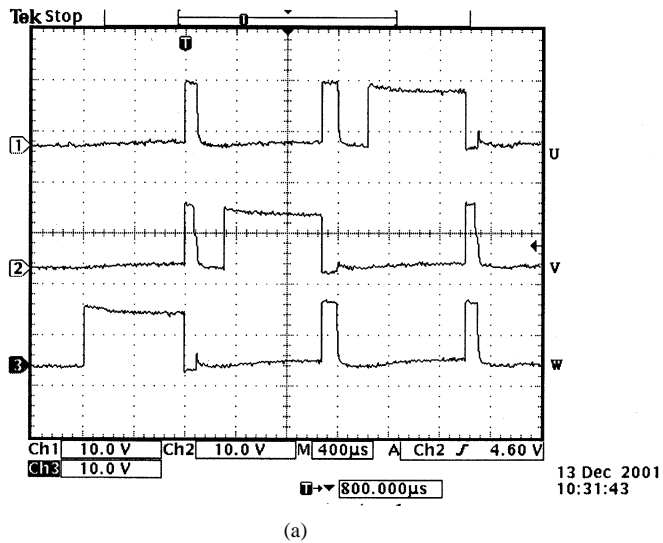


Fig. 15. Experimental results, proposed technique. (a) $A = 1$. (b) $A = 2$. (c) $A = 3$. (d) $A = 4$. (e) $A = 5$. (f) $A = 6$.

Altera Flex EPF6024AQC240-3 is used for the realization of the presented initial position detection technique. The features of this chip are shown in Table II. As shown in Table II, it has around 20 000 gates. The software is developed using the MAX+Plus II.¹ As shown in Fig. 13, power devices of the inverter are controlled according to the configuration of excitation signals shown in Fig. 10. As shown in Fig. 10, there are six time intervals, $T_1 \sim T_6$, which are identified by a 3-bit counter implemented using Altera.

Moreover, the “Excitation Signal Generator” generates the required excitation signals in “ T_1 ,” “ T_3 ,” and “ T_5 ” time intervals. In “ T_2 ” (“ T_4 ” and the “ T_6 ”) time interval, the time periods in which terminal voltages “ V_U ” and “ V_W ” (“ V_W ” and “ V_U ,” and “ V_W ” and “ V_V ”) are greater than the reference are counted by two 16-bit counters. These results are stored in 16-bit registers to give comparison results. The initial position of the permanent magnet of the rotor can, therefore, can be determined by the lookup table shown in Table I.

Note that, for the implementation, the number of 16-bit counters is only two, rather than the six shown in Fig. 13. The reason for using six 16-bit counters is only for the explanation of FPGA implementation.

B. Simulation and Experimental Results

Fig. 14 illustrates the simulation results for FPGA implementation using “ A ” = 1 as an example. As shown in Fig. 14, the excitation signals as shown in Fig. 10 can be generated by FPGA, and the correct comparison results can be derived once the terminal voltages are provided. The simulation results confirm the implementation using FPGA.

Fig. 15 illustrates the experimental results for six possible initial positions of the permanent magnet. The traces are (from top to bottom) terminal voltages of “ U ,” “ V ,” and “ W ” phases. The pulsewidth applied to stator windings for initial position detection is 800 μ s. Taking Fig. 15(a) as an example, as shown in Fig. 15(a), “ Z ” = 1 ($t_{U1} - t_{V1} > 0$) “ Y ” = 0 ($t_{W2} - t_{U2} < 0$), and “ Z ” = 0 ($t_{V3} - t_{W3} < 0$), the identification equation turns out to be “ $A = 2^2X + 2^1Y + 2^0Z = 1$.” Similar identification results as shown in Fig. 15(b)–(f) can be derived for other potential rotor positions, thereby confirming the theoretical analysis of the presented technique.

V. CONCLUSIONS

This paper has contributed to the presentation of a *simple* initial position detection technique for a BLDCM *without* using any *position* and *current* sensors. Therefore, the presented technique is very promising for *low-cost* and *high-performance* sensorless BLDCM drives.

Details of the FPGA implementation of the proposed initial position detection technique were also fully explored. Experimental results derived from the FPGA-based spindle drive system were presented. These experimental results confirm the above-mentioned features and advantages.

¹<http://www.altera.com/literature/ds/dsf6k.pdf>

ACKNOWLEDGMENT

Valuable suggestions from Dr. Y. Toba, K. Seki, and J. Wu are very much appreciated.

REFERENCES

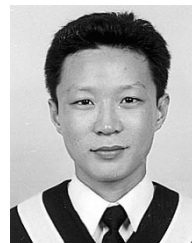
- [1] J. P. M. Bahlmann, “A full-wave motor drive IC based on the back-EMF sensing principle,” *IEEE Trans. Consumer Electron.*, vol. 35, pp. 415–420, Aug. 1989.
- [2] K. Iizuka, H. Uzuhashi, M. Kano, T. Endo, and K. Mohri, “Micro-computer control for sensorless brushless motor,” *IEEE Trans. Ind. Applicat.*, vol. IA-21, pp. 595–601, May/June 1985.
- [3] S. Ogasawara and H. Akagi, “An approach to position sensorless drive for brushless DC motors,” *IEEE Trans. Ind. Applicat.*, vol. 27, pp. 928–933, Sept./Oct. 1991.
- [4] “The smart start technique for BLDC motors—Application brief for ML4428,” Micro Linear, San Jose, CA, Sept. 1996.
- [5] A. M. Cassat, “Position detection for a brushless DC motor with sample time optimization,” U.S. Patent 4 992 710, Feb. 12, 1991.
- [6] J. C. Dunfield, “Position detection for a brushless DC motor without hall effect devices using a time differential method,” U.S. Patent 5 028 852, July 2, 1991.
- [7] HMSA, “Apparatus and method for initial position detection of permanent magnetism for three-phase synchronous motor,” Taiwan Patent pending, Jan. 2002.



Yen-Shin Lai (M’96–SM’01) received the M.S. degree from National Taiwan University of Science and Technology, Taipei, Taiwan, R.O.C., and the Ph.D. degree from the University of Bristol, Bristol, U.K., both in electronic engineering.

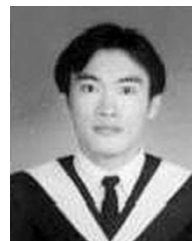
In 1987, he joined National Taipei University of Technology, Taipei, Taiwan, R.O.C., as a Lecturer. He is currently a Professor. His research interests include design of control ICs for applications of power electronics, and inverter and converter control.

Dr. Lai received the John Hopkinson Premium for the session 1995–1996 from the Institution of Electrical Engineers, U.K.



Fu-San Shyu received the B.S. and M.S. degrees in electrical engineering from National Taipei University of Technology, Taipei, Taiwan, R.O.C., where he is currently working toward the Ph.D. degree.

His research interests include inverter/converter control and circuit design.



Shian Shau Tseng received the B.S. and M.S. degrees in electrical engineering from National Taipei University of Technology, Taipei, Taiwan, R.O.C.

He is currently with Machvision, Inc., Hsin Chu, Taiwan, R.O.C. His research interests include inverter control and FPGA design.